

Photosynthesis performance, antioxidant enzymes, and ultrastructural analyses of rice seedlings under chromium stress

Jing Ma¹ · Chunfang Lv¹ · Minli Xu¹ · Guoxiang Chen¹ · Chuangen Lv² · Zhiping Gao¹

Received: 30 March 2015 / Accepted: 15 September 2015 / Published online: 23 September 2015
© Springer-Verlag Berlin Heidelberg 2015

Abstract The present study was conducted to examine the effects of increasing concentrations of chromium (Cr⁶⁺) (0, 25, 50, 100, and 200 μmol) on rice (*Oryza sativa* L.) morphological traits, photosynthesis performance, and the activities of antioxidative enzymes. In addition, the ultrastructure of chloroplasts in the leaves of hydroponically cultivated rice (*O. sativa* L.) seedlings was analyzed. Plant fresh and dry weights, height, root length, and photosynthetic pigments were decreased by Cr-induced toxicity (200 μM), and the growth of rice seedlings was starkly inhibited compared with that of the control. In addition, the decreased maximum quantum yield of primary photochemistry (*Fv/Fm*) might be ascribed to the decreased the number of active photosystem II reaction centers. These results were confirmed by inhibited photophosphorylation, reduced ATP content and its coupling factor Ca²⁺-ATPase, and decreased Mg²⁺-ATPase activities. Furthermore, overtly increased activities of antioxidative enzymes were observed under Cr⁶⁺ toxicity. Malondialdehyde and the generation rates of superoxide (O₂⁻) also increased with Cr⁶⁺ concentration, while hydrogen peroxide content first increased at a low Cr⁶⁺ concentration of 25 μM and then decreased. Moreover, transmission electron microscopy showed that Cr⁶⁺ exposure resulted in significant chloroplast damage. Taken together, these findings indicate that high

Cr⁶⁺ concentrations stimulate the production of toxic reactive oxygen species and promote lipid peroxidation in plants, causing severe damage to cell membranes, degradation of photosynthetic pigments, and inhibition of photosynthesis.

Keywords Chromium stress · Rice · Photosynthesis · Ultrastructure

Introduction

Chromium (Cr) is one of the most toxic heavy metals found in the Earth's crust. Although it is used in a variety of applications, such as electroplating, steel production, and leather tanning, it has a harmful effect on the environment (Hayat et al., 2012; Altundogan, 2005); therefore, increasingly severe environmental contamination has become a growing concern in the past several years (Zayed and Terry 2003). Previously, Cr⁶⁺ has been shown to be toxic to plants (Shanker et al., 2005), aquatic animals (Velma et al., 2009), and microorganisms (Cheung and Gu, 2007). Moreover, a Cr⁶⁺ salt was reported to have higher mobility than Cr³⁺ salt and was therefore considered to be associated with decreased plant growth and changes in plant morphology (Hayat et al., 2012). Although Cr⁶⁺ toxicity to plants is considered a major environmental problem (Sundaramoorthy et al., 2010), the mechanism underlying its action is not fully understood.

It has been shown that Cr⁶⁺ exerts a wide range of toxic effects on the growth and metabolism of plants (Shanker et al., 2004). A previous study revealed that the accumulation of Cr⁶⁺ appeared as electron-dense granules in the roots of some plants (Shanker et al., 2004); however, there is a paucity of reliable information on Cr⁶⁺ deposits in Cr stress-induced chloroplasts. Studies assessing the effects of Cr⁶⁺ on

Responsible editor: Philippe Garrigues

✉ Zhiping Gao
majingjing319@163.com

¹ Jiangsu Key Lab of Biodiversity and Biotechnology, School of Life Sciences, Nanjing Normal University, No. 1 Wenyuan Road, Nanjing210023Jiangsu, China

² Institute of Food and Crops, Jiangsu Academy of Agricultural Sciences, 50 Zhongling Street, Nanjing210014, China

chloroplast organization, which is important to understanding the physiological alterations of photosynthesis in damaged plants, are scarce. Meanwhile, Cr^{6+} stress leads to physiological disorders, with plants showing abnormal stomatal conductance, reduced intercellular space, and reduced growth and yield (Azmat and Khanum, 2005). A previous work revealed that germination of *Triticum aestivum* L. seeds was reduced under 100 mg L^{-1} of Cr^{6+} (Dey et al., 2009). In addition, Liu et al. (2008) found that Cr^{6+} exposure decreased the uptake of the micronutrients manganese, iron, copper, and zinc (Mn, Fe, Cu, and Zn, respectively) in *Amaranthus viridis* L.; however, results of these studies on the effects of Cr^{6+} on photosynthesis status are rare. Furthermore, reactions with aldehydic products of lipid peroxidation were defined as evidence of oxidative stress (Sandalió et al., 2001). The induction of reactive oxygen species (ROS) scavenging enzymes constitute an important protective mechanism, which can be used as a biomarker that reflects the affinity between antioxidative capacity and Cr^{6+} tolerance (Zhang et al., 2010). Among those, superoxide dismutase ((SOD) EC 1.15.1.1) is the first line of defense against oxidative stress. Catalase ((CAT) EC 1.11.1.6) and guaiacol peroxidase ((POD) EC 1.11.1.7) and consists of mainly eliminating hydrogen peroxide (H_2O_2) systems in plants. It has been documented that POD and CAT are increased in the Cr-sensitive mung bean after treatment with different Cr^{6+} concentrations (Rout et al., 1997); meanwhile, they decreased in Cr-tolerant cultivars (Samantary, 2002). The one which has a higher affinity for eliminating of H_2O_2 is the focus of current research against heavy metal stress, with less information available in cereal crops, such as rice (Qiao et al., 2013).

This study investigated the responses of *Oryza sativa* L. to exogenous Cr^{6+} by measuring (1) changes in poor plant growth; (2) changes in photosynthetic pigment, Cr^{6+} deposits, and chloroplast ultrastructure; (3) changes in photosynthesis and the contents of soluble protein; (4) changes in malondialdehyde (MDA), superoxide (O_2^-), and H_2O_2 content; and (5) changes in SOD, CAT, and POD activity.

Materials and methods

Plant materials and growth conditions

A hydroponic experiment was performed in the greenhouse of the Xianlin campus, Nanjing Normal University, Nanjing, China. Seeds from rice cultivar LYPJ obtained from the Institute of Food Crops, Jiangsu Academy of Agricultural Sciences, were sterilized with 3.0 % H_2O_2 for 20 min, rinsed with distilled water three times, and transferred to an incubator with a 12-h light/12-h dark photoperiod. Uniformly germinated seeds were selected and transferred to plastic pots

containing Kimura B nutrient solution. Nutrient solutions prepared with deionized-nanopure water contained 48.2 mg L^{-1} $(\text{NH}_4)_2\text{SO}_4$, 24.8 mg L^{-1} KH_2PO_4 , 18.5 mg L^{-1} KNO_3 , 15.9 mg L^{-1} K_2SO_4 , 59.9 mg L^{-1} $\text{Ca}(\text{NO}_3)_2$, 134.8 mg L^{-1} $\text{MgSO}_4 \cdot 7\text{H}_2\text{O}$, 7.45 mg L^{-1} ethylenediaminetetraacetic acid (EDTA)- Na_2 , 20 mg L^{-1} Na_2SiO_3 , 2.86 mg L^{-1} H_3BO_3 , 0.08 mg L^{-1} $\text{CuSO}_4 \cdot 5\text{H}_2\text{O}$, 0.22 mg L^{-1} $\text{ZnSO}_4 \cdot 7\text{H}_2\text{O}$, 1.81 mg L^{-1} $\text{MnCl}_2 \cdot 4\text{H}_2\text{O}$, and 0.09 mg L^{-1} $(\text{NH}_4)_6\text{Mo}_7\text{O}_{24} \cdot 4\text{H}_2\text{O}$. After 7.0 days of growth, the plants were treated with different concentrations of Cr^{6+} (0, 25, 50, 100, and 200 μM). The Cr^{6+} levels assessed in the present study were based on preliminary findings, where Cr^{6+} concentrations $>200 \mu\text{M}$ were lethal to plants. The plastic pots were then placed in a growth chamber under the conditions mentioned above for 7.0 days. All solutions were refreshed every 2.0 days, and experiments were performed in triplicate.

Plant growth

Growth was measured in terms of height, root length, fresh weight, and dry weight after 7.0 days of treatment. Dry weight was obtained after drying at 80°C until a constant weight was recorded.

Pigment content determination

The contents of chlorophyll (Chl) a, Chl b, and carotenoids as well as the Chl a/Chl b percentage were determined according to a previous study (Lichtenthaler, 1987). Chl and carotenoid (Car) were extracted using ice-cold 80 % (v/v) acetone. The extract was centrifuged at $3000 \times g$ (SIGMA 3K30, Goettingen, Germany) for 5.0 min, and absorbance of the supernatant was measured at 470, 645, and 663 nm with a UV-754 spectrophotometer (Shanghai Institute of Plant Physiology, China). Pigment contents were calculated in microgram per gram of fresh weight.

Cr^{6+} deposits and chloroplast ultrastructural observation

The leaves of the control and chromium-treated plants were cut into small pieces (approximately $0.1 \times 0.5 \text{ cm}$) and initially fixed for 2.0 h at 4.0°C in 2.5 % (v/v) glutaraldehyde in a 0.1-M phosphate buffer solution (PBS, pH 7.3), followed by post-fixation with 5.0 % (w/v) aqueous osmium tetroxide for 2.0 h. The samples were rapidly dehydrated using an ascending ethanol gradient and finally embedded in Epon 812 resin. Thin sections were obtained using an LKB-V ultramicrotome (LKB Ultrascan XL, Bromma, Sweden) with a diamond knife (LKB Products, Vienna, Austria) and stained in 2.0 % (w/v) uranyl acetate and lead citrate before examination using a Hitachi H-7650 transmission electron microscope (TEM).

Chloroplast isolation

Chloroplasts were isolated according to a method described by Ketcham et al. (1984), with minor modifications. Plant material (5.0 g) was minced and placed in a precooled mortar containing the extraction medium (50 mM Tris–HCl, pH 7.6, 5.0 mM MgCl₂, 10 mM NaCl, 0.4 M sucrose, and 0.1 % bovine serum albumin (BSA)). The homogenate was centrifuged at 1000×*g* for 2.0 min and the supernatant was recentrifuged at 2000×*g* for 2.0 min. After the supernatant was removed, the pellet was supplemented with the extraction medium and the tube slightly rotated on ice blocks to obtain a uniform suspension of chloroplasts, which was then kept in the dark on ice for use in subsequent procedures.

Photophosphorylation level, adenosine triphosphate content, and calcium-ATPase and magnesium-ATPase activities

The photophosphorylation level was measured using a luminescence meter (FG-300, Shanghai Institute of Plant Physiology, Shanghai, China) as previously proposed (Ketcham et al., 1984). Approximately 0.1 mL chloroplast suspension was added to 0.9 mL reaction buffer with 10 mM K₃Fe(CN)₆, 0.2 M tricine (pH 8.0), 20 mM MgCl₂, 20 mM Na₂HPO₄, and 20 mM adenosine diphosphate (ADP) and illuminated (50 μmol m⁻² s⁻¹) for 1.0 min; 0.5 mL 20 % trichloroacetic acid (TCA) was then added to stop the reaction. The resulting solution was centrifuged at 1000×*g* for 5.0 min, and 0.1 mL supernatant was mixed with 9.9 mL 0.02 M Tris–HCl (pH 7.5). Approximately 0.2 mL of the latter sample and 0.8 mL luciferase were mixed to determine the level of photophosphorylation.

The adenosine triphosphate (ATP) content was measured using the bioluminescence method described by Zhu et al. (2001). Calcium (Ca²⁺)-ATPase and magnesium (Mg²⁺)-ATPase activities were measured as described by Vallejos et al. (1983). To assess Mg²⁺-ATPase activity, a 0.1-mL chloroplast suspension was added to activate the solution with 0.25 M (pH 8.0) Tris–HCl, 0.5 M NaCl, 0.05 M MgCl₂, 0.05 M dithiothreitol, and 0.05 M phenazine methosulfate, and the mixture was activated by illuminating (50 μmol m⁻² s⁻¹) it for 6.0 min at 25 °C. Approximately 0.5 mL activated solution was mixed with 50 mM Tris–HCl, 2.0 mM MgCl₂, and 10 μmol ATP at pH 8.0 and 36 °C for 10 min; the reaction was stopped with 20 % TCA and centrifuged. The supernatants were used for isoelectric point determination. The Ca²⁺-ATPase activity of soluble chloroplast coupling factor was determined by essentially using the same method, except that MgCl₂ was replaced with CaCl₂.

Chlorophyll a fluorescence parameters

Chl a fluorescence was determined *in vivo* using a Handy-PEA instrument (Handy PEA, Hansatech, UK) as previously described (Perreault et al., 2011). The experiment was conducted at 10:00 a.m., with the leaves allowed to adapt to the dark conditions for at least 20 min at room temperature before measurements were taken, which allowed all the reaction centers to open. The leaves were then exposed to red light of 650 nm through LED at an excitation irradiance of 3000 μmol m⁻² s⁻¹ for 800 ms. The following parameters were calculated: maximum quantum yield of photosystem II (PSII) (*Fv/Fm*), absorption flux of photons per cross section (ABS/CS_M), phenomenological fluxes for trapping per cross section (TR₀/CS_M=φP₀ [ABS/CS_M]), potential electron transport per cross section (ET₀/CS_M=φE₀ [ABS/CS_M]), and dissipation per excited leaf cross section (DI₀/CS_M=[ABS/CS_M]-[TR₀/CS_M]). The measurements were replicated 15 times.

Protein extraction and sodium dodecyl sulfate–polyacrylamide gel electrophoresis analysis

Proteins were extracted on ice with a mortar and pestle in cool extracting medium (50 mM Tris–HCl, pH 7.6, 5.0 mM MgCl₂, 10 mM NaCl, 0.4 M sucrose, and 0.1 % BSA) and mixed with an equal volume of sodium dodecyl sulfate (SDS)-loading buffer, consisting of 10 % glycerol (*w/v*), 5.0 % mercaptoethanol (*v/v*), 2.3 % SDS, 6.25 mM Tris–HCl (pH 6.8), and 0.01 % (*w/v*) bromophenol blue (René et al., 2011). The samples were then boiled for 5.0 min, and equal amounts of protein were loaded onto 12 % polyacrylamide gel. The gel was run at 120 V, and protein bands were detected using Coomassie Brilliant Blue R-250 staining.

Determination of malondialdehyde, O₂⁻, and H₂O₂ contents

MDA contents were estimated as described by Wu et al. (2003). Leaves were homogenized in 10 % (*w/v*) TCA solution and centrifuged at 5000×*g* for 10 min. The resulting supernatant was mixed with the same volume of 0.5 % (*w/v*) thiobarbituric acid solution in 20 % (*w/v*) TCA. The mixture was then heated at 100 °C for 30 min and quickly cooled on ice. The absorbance was measured at 532 and 600 nm at 25 °C, and the concentration of MDA was expressed as micromole per gram of fresh weight (μmol g⁻¹ FW).

O₂ generation rates were measured by monitoring nitrite formation from hydroxylamine according to Wang and Luo (1990). Plant material of 0.2 g weight was homogenized in 3.0 mL of 65 mM K-phosphate buffer (pH 7.8) and then centrifuged at 5000×*g* for 10 min at 4 °C. The supernatants

(0.75 mL) were mixed with 0.675 mL of the above phosphate buffer and 0.075 mL of 10 mM hydroxylamine chlorhydrate. After incubated at 25 °C for 20 min, 0.5 mL mixture was added with 0.5 mL of 17 mM sulfanilamide and 0.5 mL of 7.0 mM α -naphthylamine and then the mixture was incubated at 25 °C for 20 min again before adding the same volume of ether. The mixture was centrifuged at 1500 \times g for 5 min. Absorbance was measured at 530 nm with the aqueous phase, and O₂ formation rates were calculated from the standard curve of NaNO₂. The results were expressed as micromole of nitrite formation per gram of fresh weight ($\mu\text{mol nitrite g}^{-1}$ FW).

H₂O₂ contents were measured according to Shen et al. (2015) by monitoring titanium sulfate. Samples (0.5 g) were homogenized with phosphate buffer (50 mM, pH 6.8) and centrifuged. The supernatants were then mixed with 0.1 % (w/v) titanium chloride in 20 % (v/v) H₂SO₄. The absorbance was measured at 410 nm, and H₂O₂ amounts were derived from the H₂O₂ standard curve. The results were expressed as micromole per gram of fresh weight ($\mu\text{mol g}^{-1}$ FW).

Activities of antioxidant enzymes

For the extraction of antioxidant enzymes, plant material (0.5 g) was homogenized on ice with a precooled mortar and pestle in 0.05 M PBS. The homogenate was centrifuged at 10,000 \times g for 20 min at 4.0 °C, and the supernatant was used to measure the activities of SOD, CAT, and POD (Fu et al., 2014). Enzyme activity assays were performed in 3.0 mL reaction volumes at 25 °C.

SOD activity was measured according to Stewert and Bewley (1980). A 3.0-mL reaction mixture was set up with 50 mM phosphate buffer (pH 7.8), 13 mM methionine, 75 mM nitro blue tetrazolium (NBT), 0.1 mM EDTA, 50 mM Na₂CO₃, and 0.1 mL enzyme extract. The reaction was started by adding 2.0 μmol riboflavin and allowed to proceed for 15 min, illuminated with two 20-W fluorescent tubes. The absorbance of the mixture was determined at 560 nm. One unit of activity was defined as the amount of enzyme required to inhibit 50 % of the initial reduction of NBT under light (unit g^{-1} FW).

CAT activity was measured at 240 nm by recording the decomposition of H₂O₂ according to Fu et al. (2014). A 3.0-mL reaction mixture was set up with 50 mM phosphate buffer (pH 7.0), 15 mM H₂O₂, and 0.1 mL enzyme extract. One unit of CAT activity was defined as the decomposition of 1.0 μmol H₂O₂ per minute per milligram of fresh weight ($\mu\text{mol H}_2\text{O}_2 \text{ min}^{-1} \text{ mg}^{-1}$ FW) at 25 °C.

POD activity was assayed according to the guaiacol method (Maehly, 1955). A 3.0-mL reaction mixture was set up with 16 mM guaiacol, 0.15 M phosphate buffer (pH 6.1), 2.0 mM H₂O₂, and 0.1 mL enzyme extract. Enzyme activity was

calculated by the increment in absorbance at 470 nm per minute per milligram of fresh weight ($\Delta\text{OD}_{470\text{nm}} \text{ min}^{-1} \text{ mg}^{-1}$ FW) at 25 °C.

Statistical analysis

Values are the mean \pm standard deviation from at least three individual experiments. The coefficients of correlation (*r* value) were calculated by using Microsoft Excel 2003. Data were assessed by one-way analysis of variance using SPSS 17.0 (SPSS Inc., Chicago, IL, USA).

Results

Cr⁶⁺ treatment of rice seedlings results in poor plant growth

Figure 1 and Table 1 show single plant fresh weight, dry weight, plant height, and root length of rice seedlings treated with increasing concentrations of Cr⁶⁺. After treating with 200 μM Cr⁶⁺, the single plant fresh and dry weights were decreased by 54.8 and 47.4 %, respectively; meanwhile, plant height and root length were decreased by 27.5 and 41.0 %, respectively.

Photosynthetic pigment, Cr⁶⁺ deposits and chloroplast development is defective in Cr⁶⁺-treated rice seedlings

Decreased Chl a ($p < 0.05$), Chl b ($p < 0.05$), and Car ($p < 0.05$) contents were observed with increasing Cr⁶⁺ levels in the nutrition medium (Table 2). In Table 2, Chl a, Chl b, Car contents, and Chl a/Chl b were decreased to 48.42, 63.58, 44.60, and 22.7 %, respectively, after treatment with increasing concentrations of Cr⁶⁺ (maximum Cr⁶⁺ concentration was 200 μM).



Fig. 1 Effects of Cr⁶⁺ stress on plant growth in rice seedling leaves

Table 1 Effects of Cr⁶⁺ on growth characteristics in rice seedling leaves

	Cr ⁶⁺ concentration (μM)				
	0	25	50	100	200
Fresh weight (g)	0.31±0.03 ^a	0.27±0.01 ^b	0.22±0.01 ^c	0.18±0.01 ^d	0.14±0.02 ^e
Dry weight (g)	0.19±0.01 ^a	0.18±0.01 ^a	0.16±0.01 ^b	0.14±0.01 ^c	0.10±0.01 ^d
Plant height (cm)	32.87±1.63 ^a	28.93±0.90 ^b	27.73±0.61 ^b	26.83±0.32 ^b	23.83±0.45 ^c
Root length (cm)	11.53±0.15 ^a	9.07±0.16 ^b	7.87±0.16 ^c	7.30±0.10 ^d	6.80±0.10 ^e

Data are mean±SD, *n*=3. Within a row, values followed by different small letters are significantly different at *p*<0.05, by using the *t* test

Transmission electron micrographs of chloroplasts under normal conditions and those of treated plants are shown in Fig. 2. There was no Cr⁶⁺ deposit in the chloroplasts of the control (Fig. 2a); however, Cr⁶⁺ deposits were found and gradually increased in plants treated with 25, 50, 100, and 200 μM Cr⁶⁺ (Figs. 2b–e).

Under normal conditions, chloroplasts are lens-shaped and intact, with an orderly arrangement of grana and stroma thylakoids. They display well-developed membrane systems consisting of grana connected by stroma lamellae (Fig. 2a). After treatment with 50 μM Cr⁶⁺, the chloroplasts swelled to an abnormal shape. When treated with 100 μmol Cr⁶⁺, their inner structure was disorganized; the chloroplast matrix zone expanded and the lamellae structure disintegrated (Fig. 2c). Higher Cr⁶⁺ concentrations increased this damage, with chloroplasts swelling even more and appearing to be globular (Fig. 2e). Finally, the inner structure of the chloroplasts was considerably disrupted.

Photophosphorylation level, ATP content, and Ca²⁺-ATPase and Mg²⁺-ATPase activities in rice seedlings are affected by Cr⁶⁺ treatment

As shown in Fig. 3, the photophosphorylation level, ATP content, and Ca²⁺-ATPase and Mg²⁺-ATPase activities overtly decreased (*r_p*=−0.983, *p*<0.01; *r_{ATP}*=−0.9478, *p*<0.01; *r_{Ca²⁺}*=−0.967, *p*<0.01; *r_{Mg²⁺}*=−0.993, *p*<0.01). After treatment with 200 μmol Cr⁶⁺, these parameters markedly

decreased, respectively, by 69.84, 68.03, 51.37, and 39.92 % compared with those of the control.

Photochemical efficiency of PSII in rice seedlings decreases after Cr⁶⁺ treatment

To further elucidate the disruption of PSII in rice seedlings exposed to Cr⁶⁺ toxicity, PSII efficiency in primary photochemistry was assessed using Chl a fluorescence. As shown in Table 3, *F_v/F_m* decreased progressively at all Cr⁶⁺ concentrations (*r*=−0.994, *p*<0.01), with a maximum loss of 45.99 % from treatment with 200 μM Cr⁶⁺; these data indicate the severe destruction of PSII reaction centers. In addition, treatment with 200 μM Cr⁶⁺ significantly reduced *ABS/CS_M* values after 7.0 days (*r*=−0.983, *p*<0.01), suggesting that high Cr⁶⁺ concentrations result in damaged antenna pigments in rice seedlings. Indeed, *DI₀/CS_M* was 16.39 % higher than that of the control after treatment with 200 μM Cr⁶⁺, indicating that the energy was dissipated as heat, and light utilization changed significantly compared with that of the control plants. In addition, *TR₀/CS_M* and *ET₀/CS_M* decreased by 19.32 and 38.96 %, respectively, under 200 μmol Cr⁶⁺.

Photosynthesis-related proteins are affected by Cr⁶⁺ treatment

The analysis of total protein extracts from the leaves of rice seedlings by SDS-PAGE showed that in Cr-treated (7.0 days)

Table 2 Effects of Cr⁶⁺ on photosynthetic pigments in rice seedling leaves

	Cr ⁶⁺ concentration (μM)				
	0	25	50	100	200
Chl a (μg g ^{−1} FW)	341.662±10 ^a	301.477±11 ^b	265.175±12 ^c	183.14±14 ^d	156.227±4 ^e
Chl b (μg g ^{−1} FW)	147.950±5 ^a	133.094±2 ^b	101.752±1 ^c	93.968±3 ^d	87.534±4 ^e
Car (μg g ^{−1} FW)	51.439±4 ^a	45.183±2 ^b	35.580±1 ^c	34.269±1 ^c	28.497±3 ^d
Chl a/chl b	2.309±0.02 ^a	2.265±0.01 ^a	2.178±0.03 ^b	1.949±0.01 ^c	1.784±0.03 ^d

Data are mean±SD, *n*=3. Within a row, values followed by different small letters are significantly different at *p*<0.05, by using the *t* test

Fig. 2 Cr⁶⁺ deposits changes in the ultrastructure of chloroplasts in leaves in control and Cr⁶⁺ treatment groups. **a, b, c, d, e** 0, 25, 50, 100, 200 μM Cr⁶⁺ concentration, respectively. *CW* cell wall, *G* Grana thylakoids, *P* plastoglobule, *SL* stroma lamellae

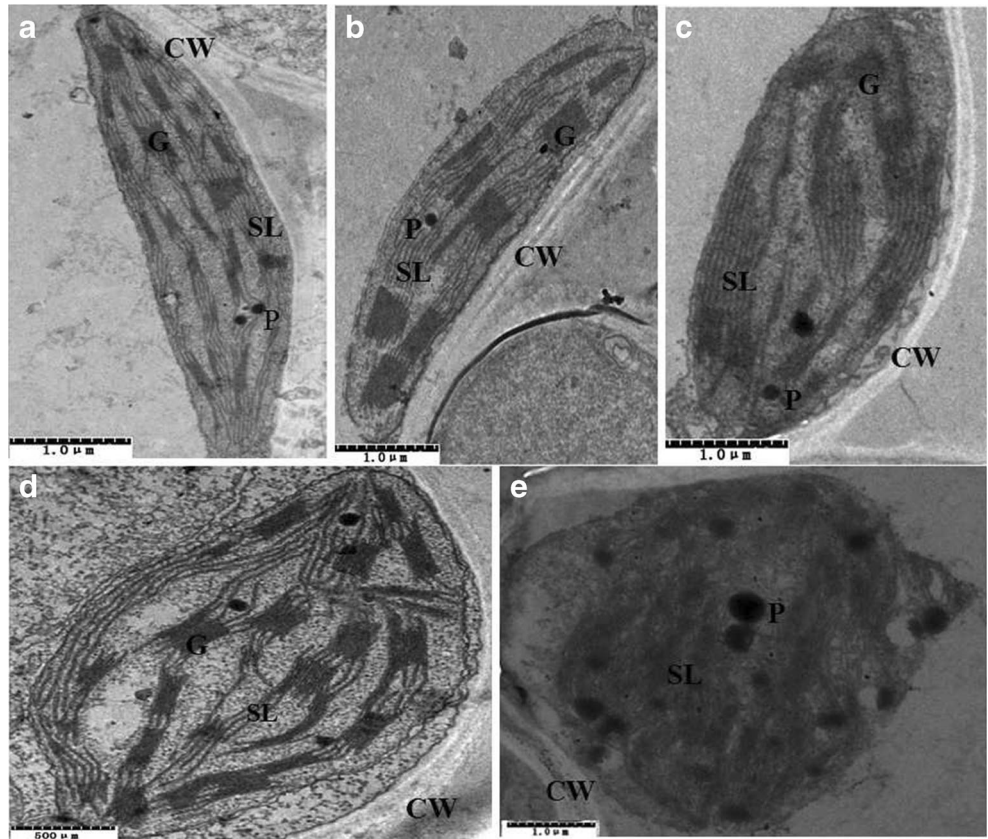


Fig. 3 Effects of Cr⁶⁺ on photophosphorylation level (**a**), ATP content (**b**), Ca²⁺-ATPase activity (**c**), and Mg²⁺-ATPase activity (**d**) in rice seedling leaves. Data are mean±SD (*n*=3). Different small letters indicate significant differences *p*<0.05, by using the *t* test

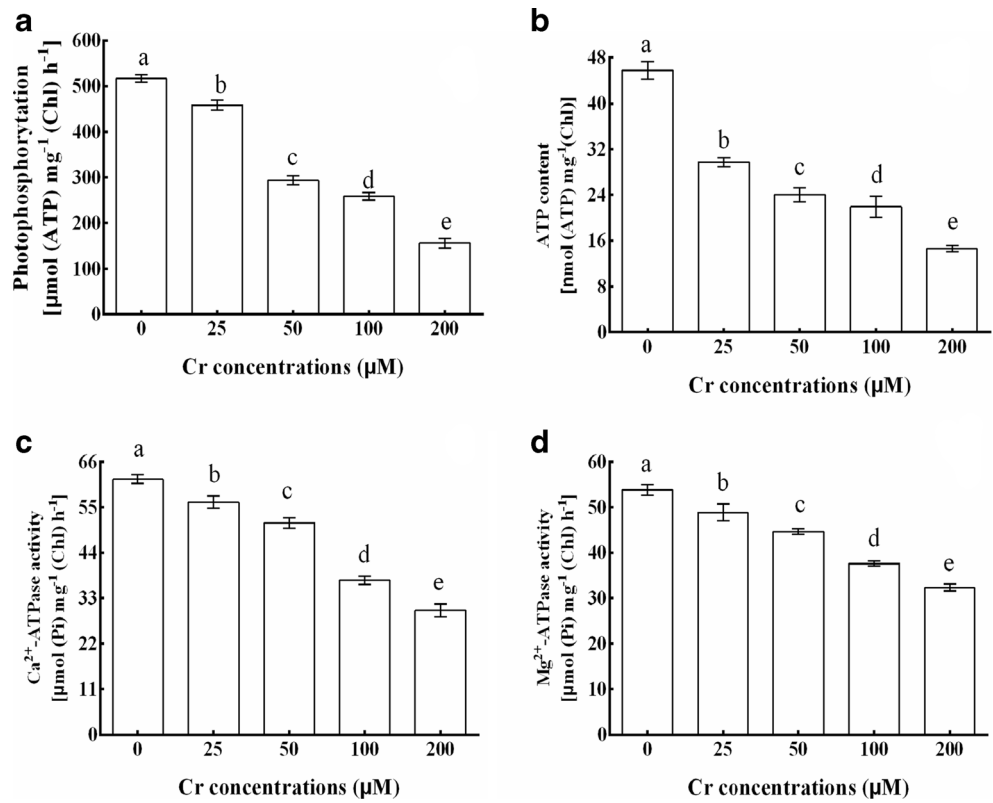


Table 3 Chlorophyll fluorescence parameters in the leaves of rice seedlings exposed to different Cr⁶⁺ concentrations

	0	Cr ⁶⁺ concentration (μM)			
		25	50	100	200
Fv/Fm	0.835±0.022 ^a	0.781±0.018 ^b	0.666±0.015 ^c	0.559±0.009 ^d	0.451±0.001 ^e
ABS/CS _M	940.22±40.84 ^a	904.33±40.32 ^b	846.00±21.02 ^c	836.11±27.18 ^c	796.56±46.10 ^d
DI ₀ /CS _M	174.50±10.08 ^a	180.67±12.32 ^b	183.78±12.10 ^c	198.44±13.13 ^c	203.11±8.43 ^d
TR ₀ /CS _M	740.67±15.87 ^a	703.67±18.93 ^b	651.00±12.00 ^c	641.33±13.78 ^d	597.56±23.24 ^e
ET ₀ /CS _M	381.50±12.95 ^a	324.88±24.64 ^b	286.00±11.53 ^c	265.88±13.32 ^d	232.88±15.74 ^e

Data are mean±SD, *n*=3. Within a row, values followed by different small letters are significantly different at *p*<0.05, by using the *t* test

leaves, exogenous Cr⁶⁺ induced a massive decrease in protein levels (Fig. 4), and protein content decreased with increasing Cr⁶⁺ concentrations. Specifically, the amounts of four polypeptides with apparent molecular weights of 43, 38, 36, and 33 kDa starkly diminished in response to Cr⁶⁺ treatment.

MDA, O₂⁻, and H₂O₂ contents in rice seedlings increased by Cr⁶⁺ treatment

The lipid peroxidation status in plants was evaluated by the MDA content. Compared with the control, treatment with Cr⁶⁺ led to a rapid increase in MDA levels in the leaves of rice seedlings (*r*=-0.989, *p*<0.01) (Fig. 5a), peaking at 53.9 % after treatment with 200 μM Cr⁶⁺. A similar trend was observed with O₂⁻ (*r*=-0.8564, *p*<0.01) (Fig. 4b), with a maximum increase of 25.2 %. H₂O₂ content (Fig. 4c) reached a peak value at 25 μmol Cr⁶⁺, which increased by 263 % over that of the control plants; however, it then declined.

Antioxidant enzyme activities in rice seedlings increased by Cr⁶⁺ treatment

Various Cr⁶⁺ stress caused pronounced effects on the activities of antioxidant enzymes in rice seedlings (Fig. 6). SOD activity was overtly changed after exposure to different Cr⁶⁺ concentrations; specifically, at 100 μM Cr⁶⁺, a significant decrease in

SOD activity was observed (Fig. 6a). CAT activity was significantly increased. There was a peak value at 100 μM Cr⁶⁺, but it was decreased with other concentrations. POD activity was increased at all concentrations except 100 μM Cr⁶⁺ (Fig. 6c).

Discussion

Cr⁶⁺ is one of the most toxic heavy metals in the environment. Several studies have assessed the chemistry of Cr⁶⁺ in soil and its uptake by plants and have concluded that it is harmful to plant growth (Arun et al., 2005). Indeed, previous studies have shown that Cr⁶⁺ toxicity in plants affects growth and development, including the germination process and growth of roots, stems, and leaves, which results in decreased total dry matter production and yield (Choudhury and Panda 2005); therefore, we evaluated Cr-treated rice seedlings for photosynthesis and ultrastructural alterations to determine the mechanism by which Cr⁶⁺ affects crops.

Ultrastructure of chloroplasts are damaged under Cr⁶⁺ stress

Our study showed that Cr⁶⁺ treatment distinctly inhibited plant growth, Chl contents, photosynthesis parameters, and chloroplast development in rice seedlings (Figs. 1 and 2,

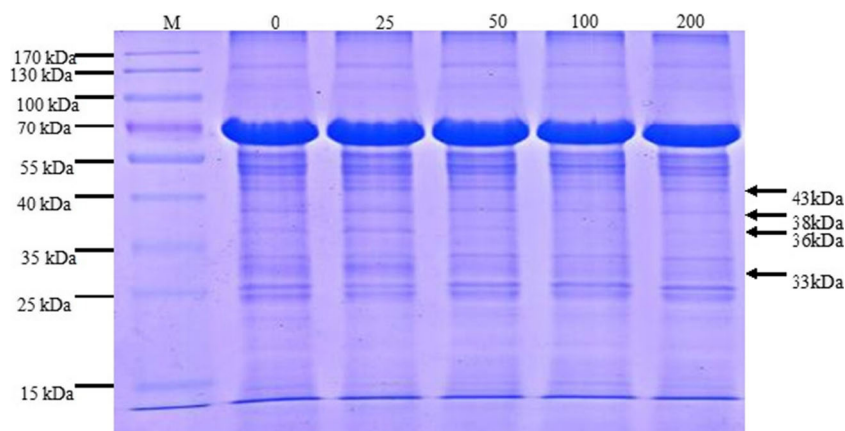
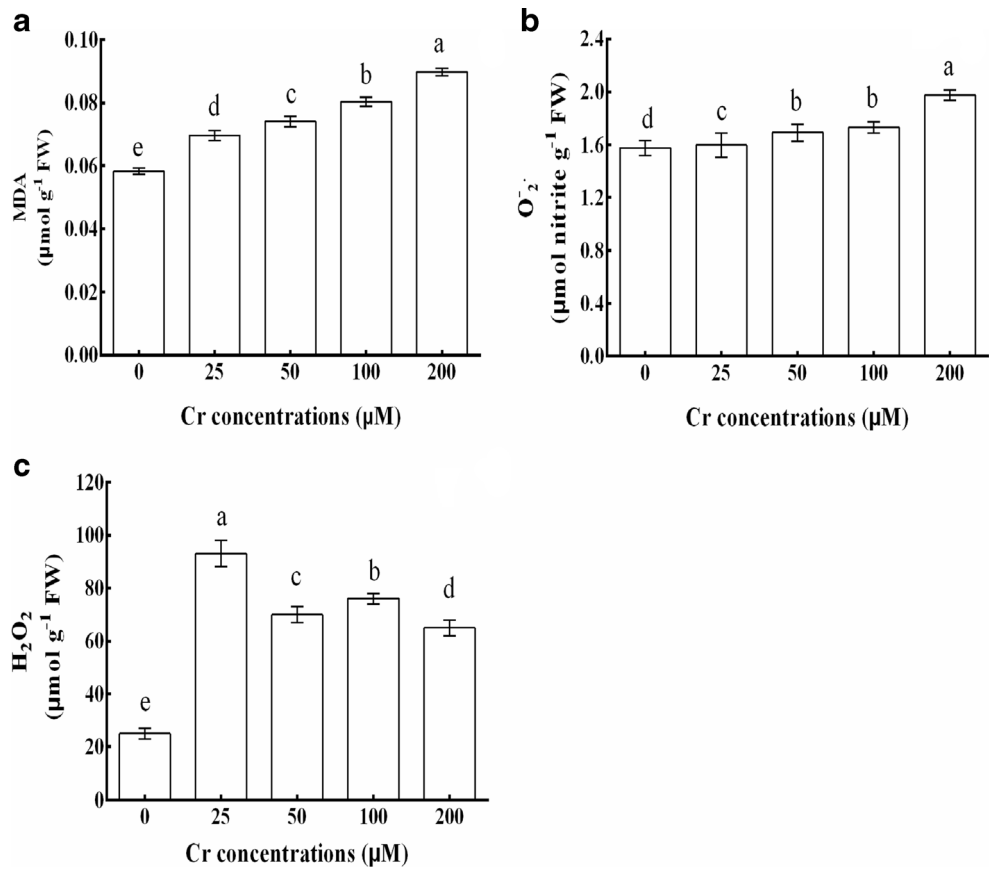
Fig. 4 Decreased protein amounts after Cr⁶⁺ treatment of leaves in rice seedlings

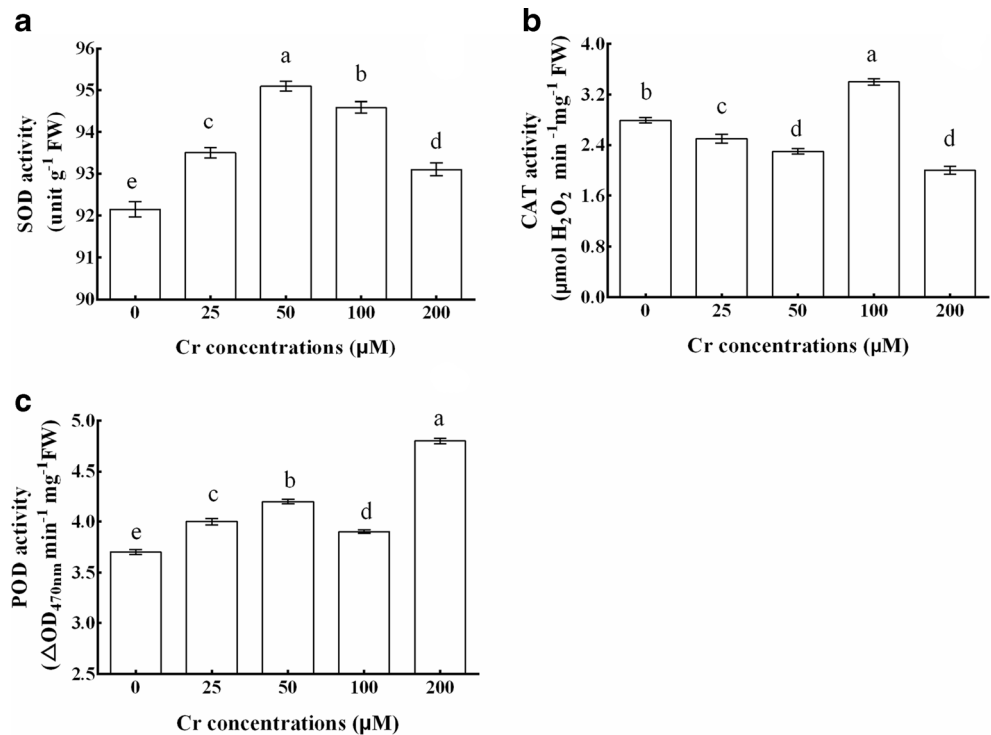
Fig. 5 Effects of Cr⁶⁺ on MDA content (a), generation rates of O₂⁻ (b), and H₂O₂ (c) in rice seedling leaves. Data are mean ±SD (n=3). Different small letters indicate significant differences p<0.05, by using the *t* test



Tables 1, 2, and 3). Photosynthetic pigment content is considered a sensitive parameter under metal stress conditions and is

used as a potential biomarker for heavy metal stress (Qiao et al., 2013). As shown in Table 2, Chl a, Chl b, and Car

Fig. 6 Effects of Cr⁶⁺ on the antioxidant enzymes SOD (a), CAT (b), and POD (c) in rice seedling leaves. Data are mean ±SD (n=3). Different small letters indicate significant differences p<0.05, by using the *t* test



contents in the leaves of rice seedlings decreased as Cr^{6+} increased from 25 to 200 μM ; similar results were obtained in *Lolium perenne* L. (Vernay et al., 2007). The decreased Chl content induced by Cr^{6+} might be a result of an inhibition of the enzymes involved in Chl biosynthesis (Singh et al., 2006; Sivaci et al., 2008). Moreover, Cr^{6+} stress induced the apparent accumulation of Cr^{6+} and significantly damaged chloroplast ultrastructure (Figs. 2b–e). Here, observations of ultrastructures showed that Cr^{6+} toxicity damages the ultrastructure of chloroplasts and thylakoids, as demonstrated by swollen chloroplasts, which were far from the cell wall, with 200 μM Cr^{6+} showing maximum severity (Fig. 2e). Photosynthesis was inevitably blocked when the integrity of the chloroplast ultrastructure in cells was destroyed under environmental stress. These changes were similar to the disorganization of the thylakoid membranes observed in *Brassica napus* L. (Gill et al., 2014).

These findings demonstrated a relationship between the structure and function of rice seedlings and that the influence of Cr^{6+} on chloroplasts was important for understanding physiological alterations. Changes in chloroplast ultrastructure were another important reason for the decrease in Chl content. Both the loss in pigment and damage to the chloroplasts ultimately cause the disturbances in photosynthetic capacity (Qiao et al., 2013).

Photosynthesis is inhibited under Cr^{6+} stress

Photophosphorylation activity is the capacity of chloroplasts to produce ATP under light conditions, using light energy to transform ADP into ATP (Zhang et al., 2007), a reaction catalyzed by ATP-synthase in chloroplast thylakoid membranes. The altered photophosphorylation activity suggests that Cr^{6+} treatment of rice seedlings decreases the capacity of chloroplasts to produce ATP and transform light energy into chemical energy (Fig. 3a). This was confirmed by the variation tendency of Ca^{2+} -ATPase and Mg^{2+} -ATPase activities (Figs. 3c, d). The decreased photosynthesis performance of Cr^{6+} -stressed seedlings might be interpreted as a decreased utilization of light energy by the treated plants toward sustaining photochemical reactions, which denotes a decrease in light-use efficiency (Wang et al., 2014). To clarify the alterations of PSII in rice seedlings treated with Cr^{6+} , PSII efficiency in primary photochemistry was assessed using Chl a fluorescence. The F_v/F_m , representing the maximum quantum yield of PSII, shows a decreasing trend with increasing concentrations of Cr^{6+} (Table 3). The decreased F_v/F_m might be a result of photo-inhibition or other injury to PSII components in rice seedlings under Cr^{6+} stress (Roháček, 2002; Rodriguez et al., 2012). A similar response was observed in ABS/CS_M , TR_0/CS_M , and ET_0/CS_M (Table 3). DI_0/CS_M markedly increased, suggesting that the energy was dissipated as heat, and the utilization of light strikingly changed

compared with those of the control seedlings. These findings corroborate a previous report by Liu et al. (2008).

Abiotic stressors, such as heavy metals, can affect plants by altering soluble protein contents (Yang et al., 2011). In the present investigation, protein contents decreased dramatically in the leaves of rice seedlings treated with ≥ 25 μM Cr^{6+} . The effect depends on the quantities as well as the types of heavy metals applied and the plants species. SDS-PAGE also revealed that Cr^{6+} treatment decreases the amount and intensity of proteins (Fig. 6). The decreased protein contents in the test plants that received higher concentrations of Cr^{6+} are most likely the result of the toxic effects of ROS (Verma and Dubey, 2003) or to the increased protease activity activated under metal stress (Xu et al., 2010). In addition, the four polypeptides with apparent molecular weights of 43, 38, 36, and 33 kDa are protein subunits of the PSII reaction center. The decrease in these four protein subunits demonstrates that the PSII reaction center is most likely damaged under Cr^{6+} stress. Ultimately, photosynthesis is inhibited.

Antioxidant enzyme systems of rice seedlings lose their intrinsic balance under Cr^{6+} stress

It is known that heavy metals cause oxidative damage resulting from the production of ROS (Malecka et al., 2001). MDA is a decomposition product of polyunsaturated fatty acids in biomembranes. It has been used as a biomarker for lipid peroxidation resulting from oxidative stress (Mittler, 2002). As shown above, when rice seedlings are subjected to elevated Cr^{6+} concentrations, MDA levels prominently increase (Fig. 5a). The increased MDA content suggests that Cr^{6+} deminifies the cell membrane and induce oxidative stress, which is shown to be related to induced production of $\text{O}_2\cdot$ and H_2O_2 (Wang et al., 2008). $\text{O}_2\cdot$ and H_2O_2 contents increase gradually with Cr^{6+} concentration (Fig. 5b, c), in agreement with previous findings (Zhang et al., 2010), which suggested that Cr^{6+} induced MDA production in wheat seedlings; therefore, membrane lipid peroxidation should be considered a component of Cr^{6+} toxicity. This effect was also evidenced by the decrease in photosynthetic pigments (Table 2) and proteins (Fig. 4). Increased MDA, $\text{O}_2\cdot$, and H_2O_2 contents result in increased oxidative and lipid peroxidation, damage the structure and function of the membranes and disturb metabolic processes, and finally inhibit the growth and physiological processes in rice seedlings. The activities of antioxidant enzymes caused by heavy metals are considered to be important defense systems of plants against oxidative stress (Zhang et al., 2010). The protective mechanisms adapted by plants to scavenge free radicals and peroxides consist of several antioxidant enzymes (POD, CAT, and SOD) (Allen, 1995). Antioxidant enzymes are important components in preventing oxidative stress, and the activity of one or more of these enzymes generally increases in plants when exposed

to toxic metals (Singh et al., 2006). SOD converts superoxide anion into another reactive intermediate (H_2O_2). In addition, H_2O_2 is removed by CAT in the peroxisomes or by membrane-bound POD (Foyer et al., 1997). The increase in SOD activities detected in the leaves of rice seedlings following Cr^{6+} treatment could be considered to be circumstantial evidence of enhanced production of free radicals. The results herein indicate that the tolerance capacity of plants to toxic metals depends on the equilibrium between the production of ROS and the quenching activity of the antioxidants (Xu et al., 2010). In addition, the activities of SOD decrease at high Cr^{6+} concentrations. It is evident from our study that the antioxidant enzyme systems of rice seedlings lose their intrinsic balance and are unable to effectively resist the generation of excess ROS. Moreover, POD is considered as having a higher capacity for H_2O_2 than CAT. In our results, the POD activity increases, except under 50 μM Cr treatment (Fig. 5c), while CAT activity is activated only at 50 μM Cr^{6+} to compensate for POD insufficiency (Fig. 5b), suggesting that CAT, not POD, might play a main role during this period, which is consistent with the previous viewpoint (Zhang et al., 2009). These relationships appear to also be connected with gene expression. Further experiments will be carried out to test this possibility.

Acknowledgments Studies in the Chen Laboratory are supported by the National Natural Science Foundation of China (Grant No.31271621/C1302), Project BK20140916 supported by NSF of Jiangsu Province of China, Program of Natural Science Research of Jiansu Higher Education Institutions of China (Grant No.14KJB180011), and a project funded by the Priority Academic Program Development of Jiangsu Higher Education Institutions. The authors thank Kaihe Du for his technical assistance with TEM.

References

Allen RD (1995) Dissection of oxidative stress tolerance using transgenic plants. *Plant Physiol* 107:1049–1054

Altundogan HS (2005) Cr (VI) removal from aqueous solution by iron (III) hydroxide-loaded sugar beet pulp. *Process Biochem* 40: 1443–1452

Arun KS, Cervantes C, Herminia LT, Avudainayagam S (2005) Chromium toxicity in plants. *Environ Int* 31:739–753

Azmat R, Khanum R (2005) Effect of chromium metal on the uptakes of mineral atoms in seedlings of bean plant *Vigna radiata* (L.) wilczek. *Pak J Biol Sci* 8:281–283

Cheung KH, Gu JD (2007) Mechanism of hexavalent chromium detoxification by microorganisms and bioremediation application potential: a review. *Int Biodeter Biodegr* 59:8–15

Choudhury S, Panda SK (2005) Toxic effects, oxidative stress and ultrastructural changes in moss *taxithelium nepalense* (schwaegr.) broth. under chromium and lead phytotoxicity. *Water Air Soil Poll* 167:73–90

Dey SK, Jena PP, Kundu S (2009) Antioxidative efficiency of *Triticum aestivum* L. exposed to chromium stress. *J Environ Biol* 30:539–544

Foyer CH, Lopez-Delgado H, Dat JF et al (1997) Hydrogen peroxide and glutathione-associated mechanisms of acclimatory stress tolerance and signalling. *Physiol Plant* 100:241–254

Fu YY, Li FF, Xu T, Cai SJ, Chu WY, Qiu H, Xu QS (2014) Bioaccumulation, subcellular, and molecular localization and damage to physiology and ultrastructure in *Nymphoides peltata* (Gmel.) O. Kuntze exposed to yttrium. *Environ Sci Pollut R* 21:2935–2942

Gill RA, Zang L, Ali B, Farooq MA, Cui P, Yang S, Ali S, Zhou WJ (2014) Chromium-induced physio-chemical and ultrastructural changes in four cultivars of *Brassica napus* L. *Chemosphere* 120: 154–164

Hayat S, Khalique G, Irfan M, Wani AS, Tripathi BN, Ahmad A (2012) Physiological changes induced by chromium stress in plants: an overview. *Protoplasma* 249:599–611

Ketcham SR, Davenport JW, Warncke K, McCarty RE (1984) Role of the gamma subunit of chloroplast coupling factor 1 in the light-dependent activation of photophosphorylation and ATPase activity by dithiothreitol. *J Biol Chem* 259:7286–7293

Lichtenthaler HK (1987) Chlorophylls and carotenoids: pigments of photosynthetic membranes. *Method Enzymol* 148:350–382

Liu D, Zou J, Wang M (2008) Hexavalent chromium uptake and its effects on mineral uptake, antioxidant defence system and photosynthesis in *Amaranthus viridis* L. *Bioresource Technol* 99:2628–2636

Maehly AC (1955) Plant peroxidase. *Method Enzymol* 12:801–813

Malecka A, Jarmuszkiewicz W, Tomaszewska B (2001) Antioxidative defense to lead stress in subcellular compartments of pea root cells. *Acta Biochim Pol* 48:687–698

Mittler R (2002) Oxidative stress, antioxidants and stress tolerance. *Trends Plant Sci* 7:405–410

Perreault F, Dionne J, Didur O, Juneau P, Popovic R (2011) Effect of cadmium on photosystem II activity in *Chlamydomonas reinhardtii*: alteration of O-J-I-P fluorescence transients indicating the change of apparent activation energies within photosystem II. *Photosynth Res* 107:151–157

Qiao XQ, Shi GX, Chen L, Tian XL, Xu XY (2013) Lead-induced oxidative damage in sterilized seedlings of *Nymphoides peltatum*. *Environ Sci Pollut R* 20:5047–5055

René VDP, Ulrike M, Georg H, Marc S, Denham EL, Monteferrante CG (2011) Environmental salinity determines the specificity and need for tat-dependent secretion of the Ywbn protein in bacillus subtilis. *Plos One* 6:589–589

Rodríguez E, Santos C, Azevedo R, Moutinho-Pereira J, Correia C, Dias MC (2012) Chromium (VI) induces toxicity at different photosynthetic levels in pea. *Plant Physiol Biochem* 53:94–100

Roháček K (2002) Chlorophyll fluorescence parameters: the definitions, photosynthetic meaning, and mutual relationships. *Photosynthetica* 40:13–29

Rout GR, Samantaray S, Das P (1997) Differential chromium tolerance among eight mungbean cultivars grown in nutrient culture. *J Plant Nutr* 20:473–483

Samantary S (2002) Biochemical responses of Cr-tolerant and Cr-sensitive mung bean cultivars grown on varying levels of chromium. *Chemosphere* 47:1065–1072

Sandalio LM, Dalurzo HC, Gómez M, Romero-Puertas MC, Delrio LA (2001) Cadmium-induced changes in the growth and oxidative metabolism of pea plants. *J Exp Bot* 52:2115–2126

Shanker AK, Cervantes C, Loza-Tavera H, Avudainayagam S (2005) Chromium toxicity in plants. *Environ Int* 31:739–753

Shanker AK, Djanaguiraman M, Sudhagar R, Chandrashekar CN, Pathmanabhan G (2004) Differential antioxidative response of ascorbate glutathione pathway enzymes and metabolites to chromium speciation stress in green gram (*Vigna radiata* (L.) R. Wilczek. cv CO 4) roots. *Plant Sci* 166:1035–1043

Shen WJ, Chen GX, Xu JG, Zhen XH, Ma J, Zhang XJ, Gao ZP (2015) High light acclimation of *Oryza sativa* L. leaves involves specific

- photosynthetic-sourced changes of NADPH/NADP⁺ in the midvein. *Protoplasma* 252:77–87
- Singh S, Eapen S, D'Souza SF (2006) Cadmium accumulation and its influence on lipid peroxidation and antioxidative system in an aquatic plant, *Bacopa monnieri* L. *Chemosphere* 62:233–246
- Sivaci A, Elmas E, Gümüş F, Sivaci ER (2008) Removal of cadmium by *Myriophyllum heterophyllum* Michx. and *Potamogeton crispus* L. and its effect on pigments and total phenolic compounds. *Arch Environ Con Tox* 54:612–618
- Stewart RR, Bewley JD (1980) Lipid peroxidation associated with accelerated aging of soybean axes. *Plant Physiol* 65:245–248
- Sundaramoorthy P, Chidambaram A, Ganesh KS, Unnikannan P, Baskaran L (2010) Chromium stress in paddy: (i) nutrient status of paddy under chromium stress; (ii) phytoremediation of chromium by aquatic and terrestrial weeds. *Cr Biol* 333:597–607
- Vallejos RH, Arana JL, Ravizzini RA (1983) Changes in activity and structure of the chloroplast proton ATPase induced by illumination of spinach leaves. *J Biol Chem* 258:7317–7321
- Verma S, Dubey RS (2003) Lead toxicity induces lipid peroxidation and alters the activities of antioxidant enzymes in growing rice plants. *Plant Sci* 164:645–655
- Vernay P, Gauthier-Moussard C, Hitmi A (2007) Interaction of bioaccumulation of heavy metal chromium with water relation, mineral nutrition and photosynthesis in developed leaves of *Lolium perenne* L. *Chemosphere* 68:1563–1575
- Velma V, Vutukuru SS, Tchounwou PB (2009) Ecotoxicology of hexavalent chromium in freshwater fish: a critical review". *Rev Environ Health* 24:129–145
- Wang AG, Luo GH (1990) Quantitative relation between the reaction of hydroxylamine and superoxide anion radicals in plants. *Plant Physiol Commun* 6:55–57
- Wang C, Wang X, Tian Y, Xue Y, Xu X, Sui Y, Yu H (2008) Oxidative stress and potential biomarkers in tomato seedlings subjected to soil lead contamination. *Ecotox Environ Safe* 71: 685–691
- Wang Y, Jiang X, Li K, Wu M, Zhang RF, Zhang L, Chen GX (2014) Photosynthetic responses of *Oryza sativa* L. seedlings to cadmium stress: physiological, biochemical and ultrastructural analyses. *Biomaterials* 27:389–401
- Wu FB, Zhang GP, Dominy P (2003) Four barley genotypes respond differently to cadmium: lipid peroxidation and activities of antioxidant capacity. *Environ Exp Bot* 50:67–78
- Xu QS, Hu JZ, Xie KB, Yang HY, Du KH, Shi GX (2010) Accumulation and acute toxicity of silver in *Potamogeton crispus* L. *J Hazard Mater* 173:186–193
- Yang YL, Zhang YY, Wei XL, You J, Wang WR, Lu J, Shi RX (2011) Comparative antioxidative responses and proline metabolism in two wheat cultivars under short term lead stress. *Ecotox Environ Safe* 74:733–740
- Zayed AM, Terry N (2003) Chromium in the environment: factors affecting biological remediation. *Plant Soil* 249:139–156
- Zhang CJ, Chu HJ, Chen GX, Shi DW, Zuo M, Wang J, Lu CG, Wang P, Chen L (2007) Photosynthetic and biochemical activities in flag leaves of a newly developed superhigh-yield hybrid rice (*Oryza sativa*) and its parents during the reproductive stage. *J Plant Res* 120:209–217
- Zhang H, Hu LY, Li P, Hu KD, Jiang CX, Luo JP (2010) Hydrogen sulfide alleviated chromium toxicity in wheat. *Biol Plantarum* 54: 743–747
- Zhang SS, Zhang HM, Qin R, Jiang WS, Liu DH (2009) Cadmium induction of lipid peroxidation and effects on root tip cells and antioxidant enzyme activities in *Vicia faba* L. *Ecotoxicology* 18: 814–823
- Zhu XY, Chen GC, Zhang CL (2001) Photosynthetic electron transport, photophosphorylation, and antioxidants in two ecotypes of reed (*Phragmites communis* Trin.) from different habitats. *Photosynthetica* 39:183–189